1 Supplementary material for LHCb-PAPER-2014-061

1.1 Discussion of possible feed-down

It should be noted that with a specific configuration of other excited Ξ_b states, it is possible to produce a narrow peak in the $\Xi_b^0\pi^-$ mass spectrum which is not due to a $\Xi_b^{\prime -}$ resonance. This can arise from the decay chain $\Xi_b^{**-} \to \Xi_b^{\prime 0}\pi^-$, $\Xi_b^{\prime 0} \to \Xi_b^0\pi^0$ where the Ξ_b^{**-} is the $J^P = 1/2^-$ state analagous to the $\Xi_c(2790)$. If the decays are close to threshold, the tracks will be kinematically correlated such that combining the Ξ_b^0 daughter with the π^- from the Ξ_b^{**-} would produce a structure in the $m(\Xi_b^0\pi^-)$ spectrum. In order for this feed-down process to produce a narrow peak consistent with what is seen in the data, several criteria must be fulfilled.

1. The process $\Xi_b^{\prime -} \to \Xi_b^0\pi^-$ must be below threshold, else an additional peak would be seen due to a real $\Xi_b^{\prime -}$. Thus, $m(\Xi_b^{\prime -}) < m(\Xi_b^0) + m(\pi^-)$.

2. The process $\Xi_b^{\prime 0} \to \Xi_b^0\pi^0$ must be above threshold but only by a small amount (approximately $2\,\mathrm{MeV}/c^2$ at most). This follows from the fact that the width of the feed-down peak increases rapidly with the Q-value yet the peak observed in data is very narrow. If the process were below threshold, the decay $\Xi_b^{\prime 0} \to \Xi_b^0\gamma$ would dominate instead and the feed-down peak would be broad; if it were more than $2\,\mathrm{MeV}/c^2$ above threshold, the feed-down peak would again be too broad. Thus, $0 < m(\Xi_b^{\prime 0}) - m(\Xi_b^0) - m(\pi^0) \lesssim 2\,\mathrm{MeV}/c^2$.

3. Combining the first two constraints it follows that $m(\Xi_b^{\prime -}) - m(\Xi_b^{\prime 0}) < m(\pi^-) - m(\pi^0) \simeq 4.6\,\mathrm{MeV}/c^2$. This is at the edge of what is plausible given the large isospin splitting measured in the Ξ_b ground state.

4. The process $\Xi_b^{**-} \to \Xi_b^{\prime 0}\pi^-$ must be exactly $3.65\,\mathrm{MeV}/c^2$ above threshold in order to reproduce the position of the peak seen in data. Thus, $m(\Xi_b^{**-}) = m(\Xi_b^{\prime 0}) + m(\pi^-) + 3.65\ \mathrm{MeV}/c^2$.

5. The isospin partner process $\Xi_b^{**0} \to \Xi_b^{\prime -}\pi^+$ must be below threshold, or a corresponding peak would be visible in the wrong-sign $\Xi_b^0\pi^+$ spectrum. Thus, $m(\Xi_b^{**0}) - m(\Xi_b^{\prime -}) - m(\pi^+) < 0$.

6. The production rate of the higher $L = 1$ state must be roughly half that of the $L = 0$ Ξ_b^{*-} resonance.

In short, in order for this explanation to work we have to invoke two additional new states and have them lie at specific masses close to, but just above their thresholds, and stipulate that production of the $L = 1$ state not be suppressed. We consider this to be contrived but are not able to exclude it with the data available.

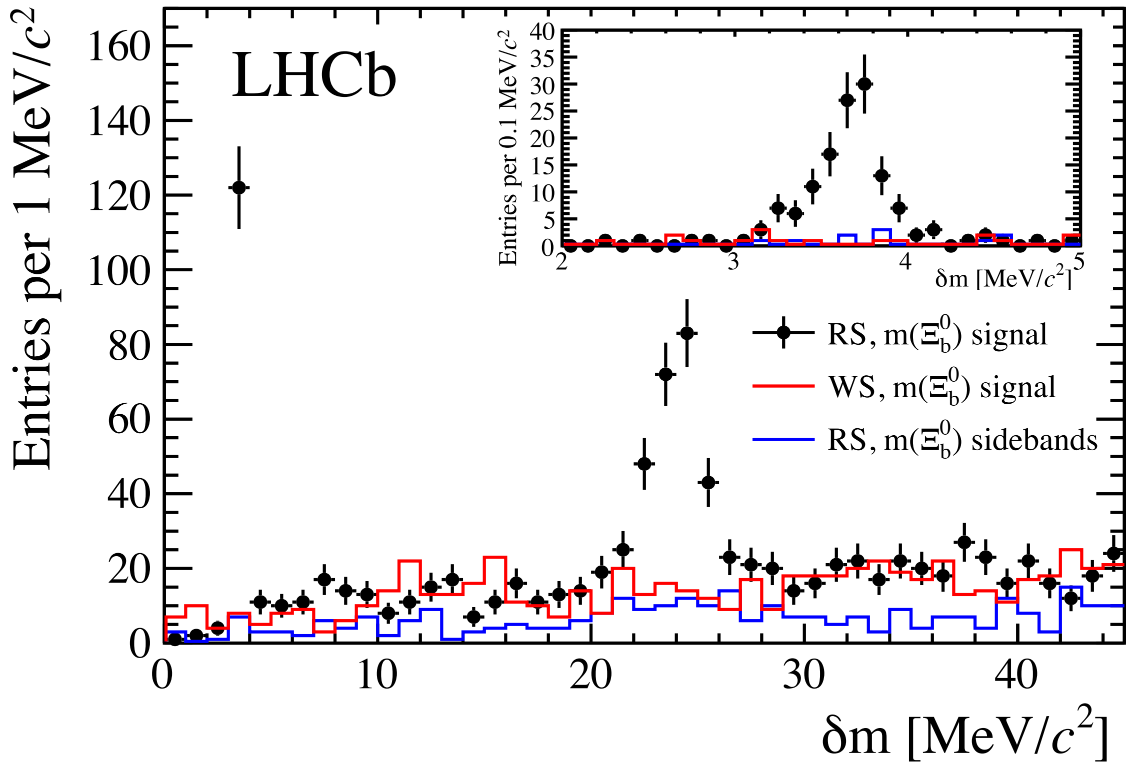

Figure 3: The δm spectra for $\Xi_b^0\pi_s^-$ candidates. The points with error bars show right-sign candidates in the Ξ_b^0 mass signal window, and the red and blue histograms show wrong-sign candidates with the same selection and right-sign candidates in the Ξ_b^0 mass sidebands, respectively. Inset: zoom of the region 2–5 MeV/c^2.

1.2 Alternative versions of plots

Fig. 3 is the alternative versions of Fig. 2 with the Ξ_b^0 mass sidebands (5715–5745 MeV/c^2 and 5845–5875 MeV/c^2) shown.

1.3 Helicity angle distributions

See Fig. 4. The data are fully consistent with a constant distribution for both peaks:

Peak	Fitted a	χ^2/NDF for best-fit a	χ^2/NDF for $a = 1$
Lower	0.89 ± 0.11	9.4/7	10.3/8
Upper	0.88 ± 0.11	3.1/7	4.4/8

A flat distribution occurs either if the resonance has $J = 1/2$ or if the resonance has $J > 1/2$ but zero longitudinal polarization. (If the polarization is small, the distribution will be nearly flat.) Therefore we cannot make any inferences about the J of the particles

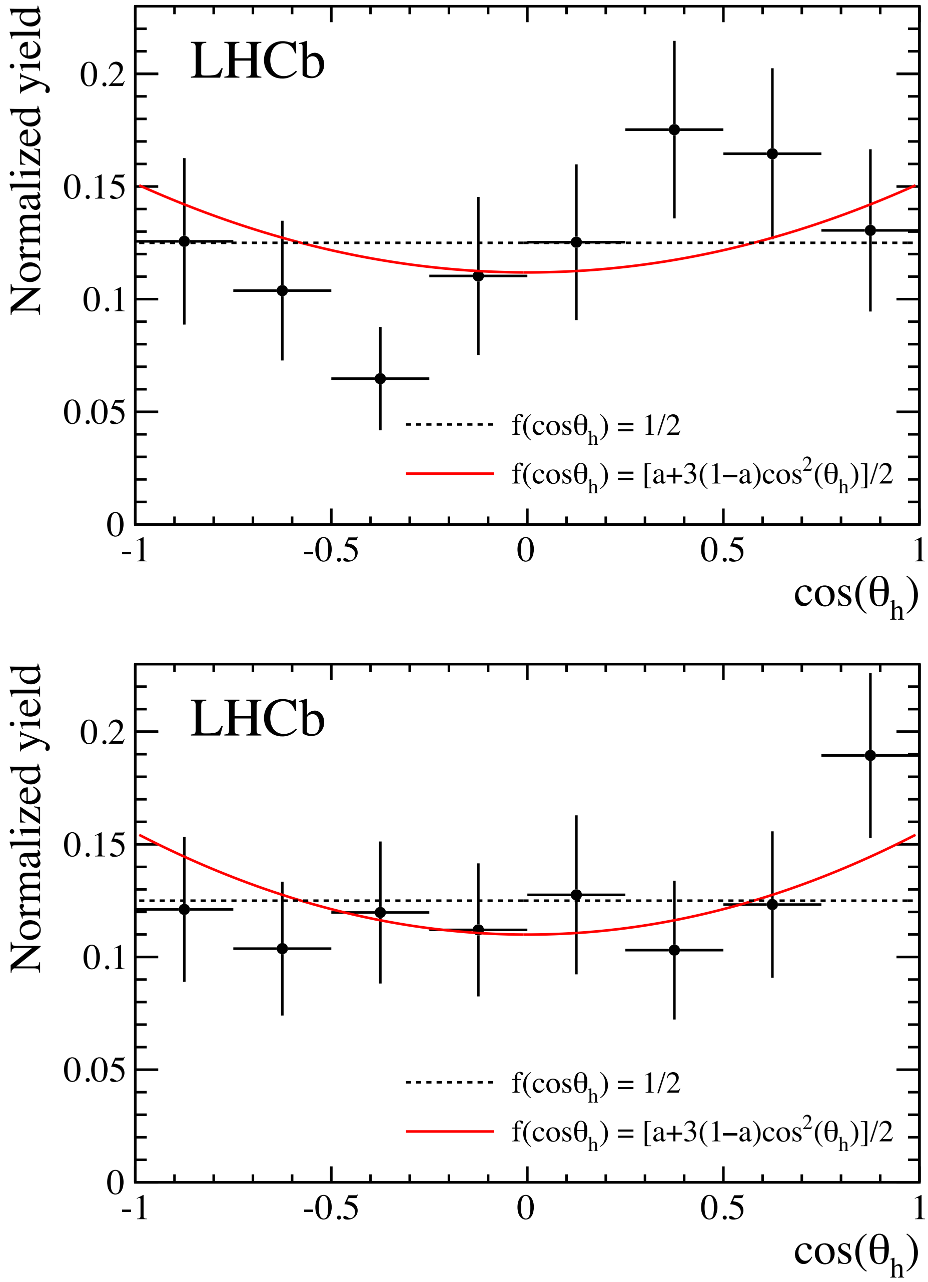

Figure 4: Fits to the $\cos\theta_h$ distributions. The dashed black line indicates a flat distribution The red curve is a fit in which a quadratic component is allowed.

with this dataset. The statement we make is: the data are consistent with the quark model predictions but other values of J are not excluded.

1.3.1 Fits for $\Xi_b^0 \to \Lambda_c^+ K^- \pi^+ \pi^-$

See Fig. 5.

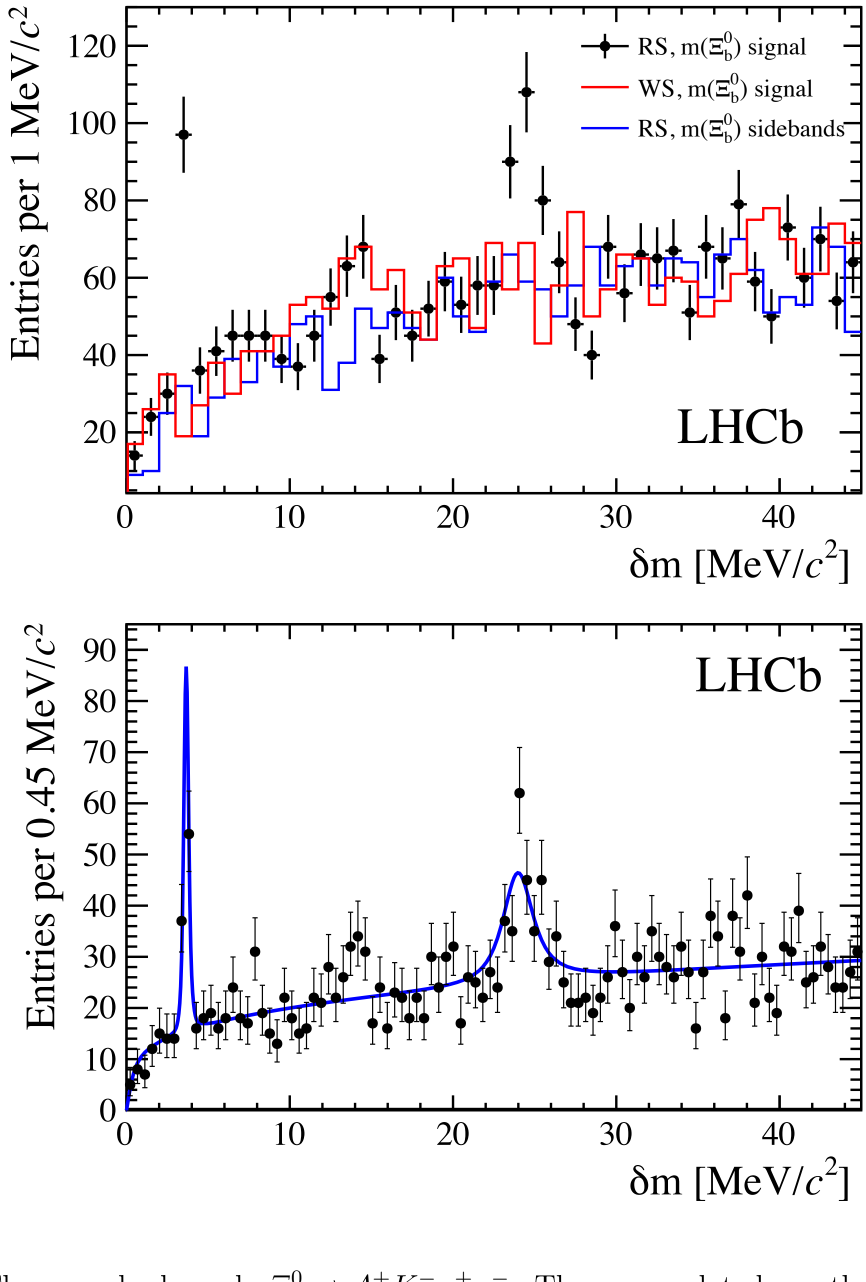

Figure 5: The crosscheck mode $\Xi_b^0 \to \Lambda_c^+ K^- \pi^+ \pi^-$. The upper plot shows the unfitted mass spectrum for right-sign $\Xi_b^0 \pi^-$ in the $m(\Xi_b^0)$ signal window (points), wrong-sign $\Xi_b^0 \pi^-$ (red histogram), and the right-sign mass sidebands (blue histogram). The lower plot shows a fit to the same right-sign data. In the fit, the masses and widths are fixed to the values obtained in the fit to the main $\Xi_b^0 \to \Xi_c^+ \pi^-$ sample. The statistical significances are 6.4σ for the lower peak and 4.7σ for the upper peak (from Wilks' theorem).

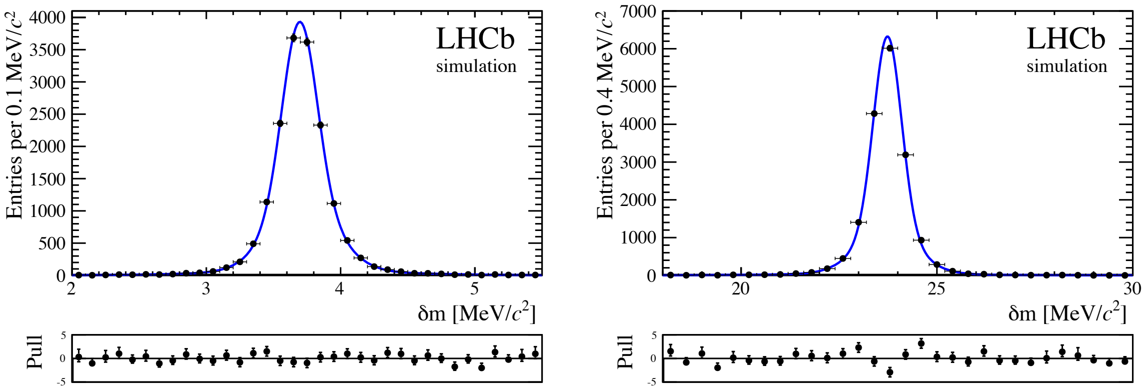

Figure 6: Samples of simulated signal events (points), fitted with a resolution function (blue curve). The normalised residuals are shown below. See Sec. 1.4 for details of the lineshape used.

1.4 Resolution functions

The resolution functions used for the two peaks are fixed with signal MC samples, one for each peak. The samples are generated with the standard LHCb simulation software. The samples consist of events of the form $\Xi_b^{*-} \to \Xi_b^0 \pi^-$, $\Xi_b^0 \to \Xi_c^+ \pi^-$, $\Xi_c^+ \to pK^-\pi^+$. For each peak, the mass of the Ξ_b^{*-} is chosen to approximately reproduce the value of δm seen in data (values of $\delta m = 3.69\,\mathrm{MeV}/c^2$ and $23.69\,\mathrm{MeV}/c^2$ are used) and the natural width is set to a value much smaller than the experimental resolution. After imposing all selection requirements and requiring a successful truth-match, yields of approximately $17,000$ candidates are found for both peaks.

The candidates are then fitted with a resolution function in an unbinned, extended maximum likelihood fit. The function chosen is the sum of three Gaussian shapes, each with a separate mean and sigma:

$$p(\delta m) = f_1\, G(\delta m, \mu_1, \sigma_1) + (1 - f_1) f_2\, G(\delta m, \mu_2, \sigma_2) + (1 - f_1)(1 - f_2)\, G(\delta m, \mu_3, \sigma_3), \quad (1)$$

where $G(\delta m, \mu, \sigma)$ is a Gaussian function with mean μ and width σ, normalised to unit integral. The fitted distributions are shown in Fig. 6. The fitted parameters are shown in Table 2. The mean of the first Gaussian is found to be offset from the input value by $+0.005\,\mathrm{MeV}/c^2$ for the first peak and $+0.049\,\mathrm{MeV}/c^2$ for the second peak; these shifts are due to a combination of momentum scale effects in the simulation and the built-in asymmetry of the lineshape.

Table 2: Parameters obtained from the resolution lineshape fits to signal MC. The yields are defined recursively, such that the yield of the primary Gaussian is $f_1 N$, the yield of the second Gaussian is $(1-f_1)f_2 N$, and the yield of the third Gaussian is $(1-f_1)(1-f_2)N$.

Parameter	First peak	Second peak	
μ_1	3.6951 ± 0.0024	23.7394 ± 0.0049	MeV/c^2
$\mu_2 - \mu_1$	0.0196 ± 0.0071	-0.0305 ± 0.0186	MeV/c^2
$\mu_3 - \mu_1$	0.0658 ± 0.0264	-0.4957 ± 0.1296	MeV/c^2
f_1	0.555 ± 0.059	0.672 ± 0.033	
f_2	0.856 ± 0.016	0.897 ± 0.013	
σ_1	0.1285 ± 0.0053	0.3544 ± 0.0088	MeV/c^2
σ_2/σ_1	1.90 ± 0.06	2.10 ± 0.07	
σ_3/σ_1	5.55 ± 0.31	6.51 ± 0.43	
Yield	16525 ± 129	17195 ± 131	